# Ecological interactions in breast cancer: Cell facilitation promotes growth and survival under drug pressure

**Authors:**

Rena Emond[1*], Jason I. Griffiths[1*], Vince Kornél Grolmusz[1*], Rachel S. Sousa[2], Andrea H. Bild[1#], Frederick R. Adler[3, 4#]

**Affiliations:**

[1] Department of Medical Oncology and Therapeutics Research, Beckman Research Institute, City of Hope National Medical Center, Monrovia, CA

[2] Department of Mathematics, Oregon State University, Corvallis, OR, 97331,

[3] School of Biological Sciences, University of Utah, Salt Lake City, UT, 84112

[4] Department of Mathematics, University of Utah, Salt Lake City, UT, 84112

* contributed equally

# To whom correspondence should be addressed: Andrea H. Bild (abild@coh.org) and Frederick R. Adler (adler@math.utah.edu)

## Abstract

The interplay of positive and negative interactions between drug sensitive and resistant cells determines the efficacy of treatment in heterogeneous cancer cell populations. We developed isogenic estrogen receptor positive (ER+) breast cancer cell lineages sensitive and resistant to ribociclib-induced CDK4/6 inhibition to investigate cell interactions under selective pressure. During treatment with ribociclib alone or in combination with endocrine therapies, sensitive cells survive and proliferate better when grown together with resistant cells than when grown in monoculture. Liquid chromatography-tandem mass spectrometry (LC-MS/MS) assays detected estrone, a less active metabolite, in medium taken from each lineage but detected highly active estradiol only from resistant cells. Because sensitive cells are more dependent on estrogen signaling than resistant cells, they benefit from the increase in local estradiol from resistant cells, leading to facilitated growth when grown under treatment in coculture. We developed a suite of mathematical models to quantify the strength of competition and facilitation between cell lines and evaluate the effects of treatments that modify these interactions. These analyses support the conclusion that resistant cell lineages facilitate growth of sensitive lineages during therapy through the increased production and sharing of local estradiol and themselves suffer from increased competition and suppression as a result. These models show that blocking facilitation has the potential to control both resistant and sensitive cell populations and inhibit the emergence of a refractory population. This combination of experiments and models shows that interactions within heterogeneous cancer cell populations can combine positive and negative interactions to shape the dynamics of resistance.

# Introduction

Cancerous tumors are heterogeneous, consisting of cells that differ both genetically and phenotypically (1). This heterogeneity creates three major obstacles for treating cancer. First, cells can have different susceptibilities to treatment, meaning that even a highly targeted and effective treatment might fail to effectively kill or inhibit some cells (2, 3). Second, this differential survival and reproduction is the natural selection that drives the continued evolution of tumor resistance to drug therapy (1, 4). For example, many breast cancers are polyclonal at multiple times during their treatment, with evolutionary trajectories showing different subclonal populations responsive or resistant to therapy (5). Despite this heterogeneity, current treatment strategies are reactive and directed at treating the resistant state after it occurs instead of developing strategies to prevent its emergence (6, 7). Novel and personalized therapeutic strategies incorporating evolutionary principles show promising results in clinical trials (8). The third challenge of heterogeneity emerges from ecology rather than evolution (9-14). Heterogeneous cell populations create the possibility for asymmetric interactions among cells that can alter responses to treatment (14, 15). Even in a homogeneous tumor, cells interact through competition for resources and space and potentially through cooperative interactions such as the production of public goods that recruit resources, suppress the immune response, or poison neighboring healthy cells (16). These interactions provide both targets and challenges for therapy, but have fewer possibilities than asymmetric interactions that could occur among heterogeneous cells, such as those sensitive and resistant to treatment (17, 18). For example, one cell type could aid the other, while suffering from competition itself (19). Such complex cell-cell interactions make predicting response to treatment much more difficult.

As in ecology, competition among cancer cells will typically reduce overall cell population size. However, competition can promote evolution of tumor heterogeneity when rare cell types with different needs or limiting factors have a growth advantage (11, 20). In contrast, cooperation in general helps support larger and more persistent populations (21-24) and can act to increase or reduce diversity depending on the specific mechanisms involved (25-27). Of most concern, cooperation may create new ways for tumors to be resistant to treatment if cells work together to survive (21, 28).

Cooperation takes on multiple types and seldom exists in isolation from competition (29, 30). For example, types that compete for resources can simultaneously benefit each other through defense against threats or enhanced access to resources. We use the term **facilitation** to describe cases where competitors of one type benefit those of another (31). For example, facilitation emerges among plants competing for water when one individual gains from water that leaks from the roots of a deeper-rooted neighbor (32). This coincidence of competitive and facilitative interactions requires detailed mathematical models to disentangle their concurrent effects and experiments to identify specific modes of competition and cooperation.

Evolutionary ecologists have defined many factors that promote the evolution and maintenance of different types of cooperation, including facilitation (25, 33-35). The stress gradient hypothesis (24), that cooperation is more likely in stressful conditions, has particular relevance to cancer. Spatially explicit models indicate that cooperation is more likely to persist in regions of high stress, such as cells undergoing drug treatment, where cooperative benefits outweigh the negative effect of competition for resources (36). This clonal cooperation can be maintained through many

interactions such as cell-cell physical communication and paracrine effects (37). Differential production of growth factors among heterogenous subclones, such as increased FGF2 in afatinib-resistant lung cancer cells and IL-11 and FIGF in polyclonal breast cancer, has been linked to acquisition of resistance (38).

This study explores the dynamics of competition and facilitation in breast cancer. This common cancer is classified into three main subtypes with hormone receptor-positive tumors, including estrogen and progesterone receptors, making up 75% of cases (39). Tumors of ER+ breast cancer are polyclonal and heterogeneous, with cells of different levels of estrogen receptor expression and different levels of estrogen addiction co-existing (5), but with unknown strength of cooperation and competition among cell types. Interestingly, endocrine therapy is given as primary treatment even if a patient's tumor shows just 1% estrogen receptor (ER) expression because these patients often respond despite the heterogeneity (40). This cross-talk exemplifies the interconnectedness of tumor population (25).

Endocrine therapies are estrogen antagonists that either deplete estrogen, made endogenously or by breast cancer cells (aromatase-inhibition), or block ER activity through modulation or degradation (5, 41, 42). At least 33% of patients with early-stage disease will develop endocrine resistance, increasing to approximately 90% of patients with metastatic disease (43, 44). The combination of endocrine therapy with cyclin-dependent kinase (CDK) 4/6 inhibitors of the cell cycle has improved disease control in metastatic ER+ breast cancer. Adjuvant trials are underway to study the efficacy of this combination in early-stage, non-metastatic breast cancer (45-50).

To investigate the type, strength and mechanism of cell interactions in heterogeneous cancer populations during selective pressure, we developed ER+ breast cancer cell lineages that are sensitive or resistant to CDK4/6 cell cycle inhibition (ribociclib). The influence of treatment on cell-cell ecological interactions was revealed by fitting mathematical models of population growth, including logistic and Lotka-Volterra models, to observed monoculture and coculture growth trajectories of resistant and sensitive populations grown with or without treatment. Resistant cells were found to facilitate sensitive cancer cell survival during drug treatment, and further experiments show that the source of the facilitation is estradiol. Extended experiments and modelling show that modification of estradiol and cellular estrogen signaling impacts the facilitative signal from resistant cells and the growth of sensitive cells. Examining mono- and coculture growth trajectories across a broader range of drug doses we parameterized a mechanistic model of facilitation. This consumer-resource model reveals how and when facilitation impairs cell cycle inhibition therapy and how facilitation modification could be used to jointly control resistant and sensitive populations. Our experiments and models analyze the ecological interactions of different cancer cell types under a range of treatment challenges and unravel their potentially asymmetric competitive and cooperative effects to quantify competition and cost of resistance in breast cancer, identify the mechanisms and conditions by which resistant cells facilitate the growth of sensitive cells, and predict how to manipulate cell interactions to control growth.

# Results

## Sensitive and resistant cell growth and treatment effects

We developed an *in vitro* model to study ER+ breast cancer cell interactions under selective drug pressure (see Methods). To generate isogenic lineages, we applied drug treatment to cell cultures for an extended timeframe until resistance developed compared to control drug sensitive parental lineage not exposed to treatment. These resistant and sensitive lineages, derived separately from the CAMA-1 and MCF7 ER+ breast cancer cell lines, were then labeled with lentivirus to express a fluorescent protein for monitoring each population's growth when cocultured. As shown, when grown as 3-dimensional spheroids in monoculture, untreated sensitive CAMA-1 cell populations grew more quickly than resistant cells, while under both 200nM and 400nM concentrations of ribociclib, resistant cells grew more quickly than sensitive cells **(Fig. 1a).** Measurement of these growth rates showed that sensitive cell proliferation decreased with an increase in the ribociclib concentration whereas resistant cells were much less impacted by treatment **(Fig. 1b)**. In a second ER+ breast cancer line, MCF7 **(Fig. 1c)**, the resistant cell population grew more quickly than sensitive cells, even without therapy, indicating the lack of an often-assumed cost of resistance. However, resistant cells continued to grow under therapy, while even the lowest drug dose effectively halted the growth of sensitive cells **(Fig. 1d)**. Despite these differences in the untreated setting, resistant cells of both cell lines showed a greater ability to tolerate treatment.

## Ribociclib therapy tolerance provided by facilitation of sensitive cells by resistant cells

To investigate whether cell interactions alter response to therapy, we cocultured sensitive and resistant cells under different treatments and compared growth of each population over 18 days to growth in monocultures. Cocultures were initiated in the following proportions: CAMA-1 = 50% sensitive + 50% resistant; MCF7 = 90% sensitive + 10% resistant to adjust for the higher growth rate).

To identify how treatment impacts interactions between resistant and sensitive cells, we compared each population's growth in treated coculture with the expected population trajectories from a Lotka-Volterra competition model **(Fig. 2a**) (51). We treat the combination of treatment and co-culture as a factorial experiment (see Methods for details), and use the model to derive their joint effect in the absence of an interaction (Expected combined effect) and compare with observed growth in treated monoculture (Observed combined effect). In this case, the deviation of observed treated cocultured cell growth curves from expected growth indicates facilitation.

With CAMA-1 cells, treatment with 200nM and 400nM ribociclib concentrations inhibited growth of sensitive cells more than resistant cells in monoculture (**Fig. 2b**), consistent with results in **Fig 1**. However, sensitive cells proliferated better when cocultured with resistant cells. The excess of sensitive cells in coculture at the conclusion of growth occurred even though half of the total initial

number of sensitive cells in coculture was plated in order to achieve the initial 50%-50% population.

Using the competition model, we found that sensitive cells strongly suppress resistant cells in untreated CAMA-1 cocultures, with a competitive effect 50% larger than that of resistant cells on themselves (scaled to 1.0 in these models). In contrast, resistant cells had almost no detectable competitive effect on sensitive cells (**Fig. 2c**). In ribociclib treated coculture, the null model predicts that sensitive cells will grow slightly more slowly than in treated monoculture due to competition, but we instead observed markedly increased growth showing facilitation of sensitive cells by resistant cells (**Fig. 2d**). Reciprocally, resistant cells grew more slowly than expected in treated coculture, due to the increased suppression by the sensitive cells they facilitate.

Similar to CAMA-1 cells, in MCF7 cells, sensitive monoculture growth was inhibited under 1.5uM or 2.4 uM ribociclib drug treatment, while resistant cells displayed higher drug tolerance and better survival **(Fig. 2e)**. MCF7 cells thus showed resistance despite a lack of measurable costs in monoculture, a result that carried over to coculture experiments where we saw competitive asymmetry opposite of that in CAMA-1 cells; resistant cells strongly suppressed sensitive cells in untreated cocultures while sensitive cells produced no detectable competitive effect on resistant cells (**Fig. 2f**). Despite these differences, we observed facilitation of sensitive cells by resistant, although with smaller magnitude than in CAMA-1 cells (**Fig. 2g**). Although the models identify facilitation of resistant cells by sensitive cells, the model fits are less reliable because the initial cell number is far below that fit by the monoculture model.

## Mechanisms of facilitation under ribociclib treatment

To determine the mechanisms driving facilitation during ribociclib treatment, we conducted a series of additional experiments on CAMA-1 cells. First, we tested whether resistant cells metabolize ribociclib more effectively than sensitive cells, reducing the ribociclib concentration within the media and allowing increased proliferation of cocultured sensitive cells. Using an optimized HPLC/MS method, we found that the ribociclib concentration was not decreased in media incubated with resistant spheroids more than with sensitive spheroids and that ribociclib remained at high doses (Supplementary Figure 1).

Alternatively, ribociclib resistant cells may release signaling molecules that enhance the growth of sensitive cells under drug treatment. To test this hypothesis, we compared proliferation of sensitive cells when supplemented with conditioned media transferred from spheroids of different compositions (100% sensitive, 50%-50% sensitive/resistant, 100% resistant) with or without treatment (0 or 400nM ribociclib). Conditioned media originating from spheroids containing resistant cells increased proliferation of sensitive cells significantly more than conditioned media produced by sensitive cell spheroids, with the largest benefit from cells that were themselves treated **(Fig. 3a)**, indicating that resistant cells secrete signaling molecules that provide pro-growth benefits for sensitive cells under drug pressure.

We also tested whether exosomal transfer of pro-growth elements produces the facilitation. Spheroids of 100% sensitive or 100% resistant cells were treated with or without 400nM ribociclib treatment. Exosomes were isolated from these different media settings and supplemented back into the media of untreated or 400nM ribociclib treated sensitive monoculture spheroids. Comparison of the proliferation of cells measured by spheroid area and cell count under different supplemented conditions identified no effect of exosomal transfer on sensitive cell growth under treatment (Supplementary Figure 2). These experiments indicate that a pro-growth factor secreted in the media of resistant cells under drug pressure, and independent of extracellular vesicle transfer, may mediate the facilitation of sensitive cells by resistant cells.

To identify the molecules secreted by resistant cells and responsible for promotion of sensitive cell growth under drug pressure, we measured the concentrations of a broad range of hypothesized growth-promoting factors in the media of cultured spheroids. Custom multiplex cytokine analysis for detection of other growth factors of interest (TGFβ 1-3, TGFα, EGF, and FGF2, FGF21, FGF23) showed no significant differences in levels between untreated and ribociclib treated conditions of the monoculture of sensitive cells or coculture of sensitive and resistant cells (Supplementary Figure 3a and 3b). However, the estradiol concentration significantly differed between resistant and sensitive spheroids. We used liquid chromatography-tandem mass spectrometry (LC-MS/MS) assay to detect estrone (Supplementary Figure 3c) and estradiol concentration under no treatment or 400nM ribociclib treatment **(Fig. 3b)**. Estradiol was not detectable in media from 100% sensitive cell cultures in either treatment while samples from cultures containing resistant cells showed measurable levels. Estradiol production and uptake by resistant and sensitive cells was estimated by fitting a Michaelis-Menten model (51) and accounting for limits of detection (Supplementary Information). Resistant cells are estimated to produce approximately 8 times more estradiol and use only 2.5 times more than sensitive cells **(Fig. 3c)**, generating a substantial source of the growth-promoting hormone. This result further supports estradiol secretion by resistant cells as a leading mechanism promoting growth of sensitive cells in coculture under ribociclib.

We investigated this proposed mechanism by adding estradiol or one of three ER antagonists (fulvestrant, tamoxifen, and raloxifene) to the cell culture medium and assessing growth in cells in monoculture **(Fig. 3d)**. Estradiol increased the growth of sensitive cells and decreased that of resistant cells. Similarly, three ER antagonists were tested, and both fulvestrant and tamoxifen reduced the growth of sensitive cells more than resistant cells, indicating that sensitive cells depend strongly on the ER pathway for growth. Raloxifene, a less potent endocrine pathway modulator, had no differential effect on the cell lines.

To test for interactions between treatments, monocultures of sensitive and resistant cells were treated with combination therapy of ribociclib and one of the estrogen pathway modifiers. We developed a null model of our expectation for monoculture growth without facilitation, multiplicatively incorporating the effects of the two treatments (see Methods). Estradiol addition to ribociclib treated monocultures caused sensitive cell to grow more than expected, replicating the effect of facilitation seen in coculture, while resistant cells showed no significant deviation. As expected given the potency of the combination treatment, when pooled, the three ER antagonists

show a synergistic interaction with ribociclib, reducing the growth of both cell types more than expected, and more strongly impacting sensitive than resistant cells **(Fig. 3e)**. Despite the distinctive responses of the two cell types to the three ER antagonists individually, we find consistent synergistic responses and diminished growth of sensitive cells while in culture with resistant cells **(Fig. 3f)**.

## Modifying the endocrine signaling pathway affects facilitation

Applying ribociclib treatment in coculture revealed facilitation of sensitive cells by resistant cells. Likewise, treating monocultures with estrogen pathway modifiers indicates that excess estradiol can facilitate sensitive cell evasion from the effects of treatment. To further demonstrate that estrogen signaling is involved in facilitation, we tested the effects of estrogen pathway modifiers on cells in coculture, both with and without ribociclib treatment.

Across all modifier spheroid experiments (**Fig. 4a-4d, top row**), sensitive cell proliferation was enhanced when cocultured with resistant cells compared to growth in monoculture, supporting previous findings of facilitation. To determine the generality of facilitation, we tested whether coculture alters growth in the presence of each modifier (estradiol and ER antagonists) without ribociclib. Estradiol treatment alone increased the growth of sensitive cells in untreated coculture beyond that predicted by the null model, consistent with sensitive cells being more dependent on estradiol signaling. However, we found growth of sensitive cells were not significantly increased in ribociclib treated coculture with added estradiol (**Fig. 4a**). This result is likely due to saturation of estradiol provided by resistant cells. With treatment of ER antagonists alone, sensitive cells are in general facilitated by resistant cells, most strongly with fulvestrant, moderately with raloxifene, and with no significant effect with tamoxifen (**Fig. 4e)**.

Finally, after assessing each modifier alone, we ask whether the synergy seen with the combination of estrogen pathway modifiers and ribociclib is also impacted by facilitation in coculture, which we term facilitation modification. Combining estradiol with ribociclib resulted in similar growth dynamics for sensitive cells both in monoculture and coculture, with little effect on the strength of facilitation (**Fig. 4a**). When ribociclib was combined with ER antagonists, facilitation of sensitive spheroid growth was generally increased, least of all with tamoxifen (**Fig. 4b)** but more strongly with fulvestrant (**Fig. 4c)** and raloxifene (**Fig. 4d**). To precisely quantify these effects, we compare observed growth with a null model that assumes no facilitation modification. For sensitive cells, we observe little facilitation modification by estradiol and a relatively weak effect of tamoxifen. With fulvestrant and to a lesser extent raloxifene, we see stronger facilitation modification than expected, consistent with the fact that resistant cells facilitate sensitive cell growth to both ribociclib and these two ER antagonists (**Fig. 4f**).

## Identifying and measuring the role of facilitation

To further explore the mechanism of facilitation, we used more detailed mechanism-based stage-structured consumer-resource differential equation model that treats cell growth and death

separately and includes specific functional forms for the effects of ribociclib and estradiol **(Fig. 5a)**. The detailed model of the mechanism of facilitation accurately describes the growth of resistant, sensitive and coculture spheroids under a broad range of drug doses **(Fig. 5b)**. The fitted facilitation model also quantifies how biological processes differ between resistant and sensitive cells **(Fig. 5c)**. Resistant cells were found to be approximately 60% as competitive ($\alpha$), consistent with the 1.5 times higher competitive effect of sensitive cells (**Fig. 2b**). Because we did not measure estradiol directly, we cannot separately identify the parameters associated with production and uptake, and instead a net production of estradiol ($\gamma$) by resistant cells was measured which is approximately twice that of sensitive cells, again consistent with the ratio of production/use estimated directly (8.0/2.5 = 3.2, **Fig. 2c**). In the absence of treatment, the less competitive resistant cells had a lower baseline division rate ($r$) (50% that of sensitive cells) and a lower quiescence rate ($\lambda$). However, they were far less sensitive to the cell cycle inhibitory effects of ribociclib ($k$), allowing their spheroids to continue to grow at high doses.

Next, we compared alternative models describing hypotheses about the processes underlying the interaction between resistant and sensitive cells **(Fig. 5d)**. This approach included comparisons to simpler dynamical models to verify that alternative mechanisms of cell growth could not generate the observed spheroid growth trajectories, thereby guarding against overfitting (detailed model description provided in Supplementary Information). Specifically, we constructed models based on principles of direct competition for resources (Competition alone model) or of phenotypic plasticity in which cells transition from a naive to a resistant state either in response to drug induction (Plasticity DI) or via random switching (Plasticity RS). Based on model comparison, using Watanabe–Akaike information criterion (WAIC) to penalize for the complexity of our Bayesian models (52), we found that models incorporating facilitation greatly outperformed (lower penalized prediction error) models of competition alone and models of phenotypic plasticity, either through drug induced (DI) or random switching (RS) of phenotypic states (see Methods).

Furthermore, simpler facilitation models assuming equivalent facilitation by resistant and sensitive cells (Facilitation symmetric 1-State) were greatly outperformed by facilitation models in which resistant cells contribute disproportionately to the production of facilitation factors (asymmetric facilitation models (Facilitation 1/2/3-State) vs Facilitation symmetric 1-State). Describing the cell cycle inhibitory mechanism of action of ribociclib through the addition of quiescent and senescent cell states further improved model accuracy compared to simpler models in which ribociclib simply reduces cell division rates (Facilitation 2/3-State vs Facilitation 1-State). These additional states allow the prediction of the delayed impacts of therapy at higher doses (reducing penalized prediction error) and also the estimation of the rate of division and quiescence with and without therapy. Describing cells as transitioning through proliferative, quiescent and senescent states during the cells life (Facilitation 3-State; model schematic in **Fig. 5a**) yielded a superior description of the data after penalizing for model complexity compared to the slightly simpler model with just a proliferative and joint quiescent/senescent sate (Facilitation 2-State).

We used the fitted model to predict the impact of therapeutically blocking facilitation on the growth of sensitive and resistant cell coculture populations. In the model, the binding of the facilitation factor to its specific cellular receptor ($\mu$) was reduced by differing degrees, reflecting

exposure to different doses of a receptor blocking drug such as fulvestrant. In the absence of facilitation blocking, the facilitation model accurately predicts the final resistant and sensitive cell population size (**Fig. 5e**; points show observed final cell counts at day 21, black line + yellow overlay shows model predictions under the experimental conditions). Consistent with our experimental observations (**Fig. 4b-d**), blocking facilitation factor binding was predicted to reduce the final resistant and sensitive cell population sizes across all ribociclib doses. However, facilitation needed to be reduced by more than 50% before substantial reductions in spheroid growth were predicted. This result suggests that sufficiently large amounts of estradiol were being produced to saturate the growth benefits of facilitation and that a large fraction of this signal must be inhibited for facilitation blocking to be effective. At lower ribociclib doses (<500nM), facilitation blocking caused a more severe reduction in the abundance of sensitive than resistant cells. The greater susceptibility of sensitive cells reflects the ability of the resistant cells to pre-empt access to estradiol. This is consistent with the small observed growth benefit resistant cells experience under combination treatment with ribociclib and estradiol (**Fig. 3f**).

Finally, we assessed the importance of facilitation relative to competition for resources in determining the rate of spheroid growth throughout treatment **(Fig. 5f)**. Across a broad range of ribociclib doses (<600nM) we identified a window of time during spheroid growth when facilitation was many times more important than competition. This period followed the accumulation of a sufficient population size to generate high levels of facilitation factors but ends prior to the spheroid reaching its maximal density and becoming regulated by resource limitation. At moderate ribociclib doses (200-600nM), the facilitation window shifts later into the treatment, as cell abundances increase more slowly, and the window also extends for a longer duration. At the highest ribociclib doses (>600nM), the window of facilitation closes completely. At these doses the coculture spheroid shrinks during treatment, preventing the growth of a population sufficient to produce enough facilitation factor to overcome treatment.

## Discussion

We developed *in vitro* model systems to investigate how clonal cooperation impacts the growth of heterogeneous ER+ breast cancer populations. Using cells resistant and sensitive to ribociclib (CDK 4/6 cell cycle inhibitor), we compared cell population growth in monoculture and in coculture across different treatment backgrounds and used mathematical models to unravel the contributions of treatment effects, competition, and cooperation. We showed that in 2-D culture, ER-positive breast cancer cells that are resistant to ribociclib secrete a soluble factor, most likely estradiol, that is necessary and sufficient to decrease the effect of ribociclib on drug-sensitive ER-positive breast cancer cells. Mathematical models that include facilitation fits the data better than alternative ecological models. Facilitation is expected to be evolutionarily stable when it provides reciprocal net benefits to both the facilitator and the facilitated party (53). Over the long term, it is expected that facilitation should shift away from the asymmetric benefit observed here, as the facilitators evolve to pre-emptively access the facilitation factor that they produce (54).

A key finding is that blocking facilitation has the potential to control both resistant and sensitive cell populations and inhibit the emergence of a refractory population. This may explain why ribociclib is more effective when combined with antiestrogen therapy than as monotherapy. It also predicts that treatment strategies to further decrease facilitation factors will prolong the benefits of ribociclib.

The ability to make quantitative predictions about the impacts of estrogen antagonists on heterogeneous cancer populations that accurately reflect experimental findings, based on the drug's mechanism of action, shows the potential power of developing molecular mechanism models to guide treatment strategies. It also shows that models can scale from the molecular to cancer population level, by coupling compartmental molecular kinetics models (52) with approaches from population ecology, such as consumer-resource (55) and stage-structured models (56). Our dynamical models highlight that the contribution of facilitation to proliferation and cancer population growth is not constant but shifts during the growth of the cancer. As cell abundance increases, facilitation-driven growth diminishes as carrying capacity is reached, due to an increase in resource competition. This shift suggests that competitive ability may be more essential at later stages in disease progression, while cooperation may be more important in earlier stages. Facilitation is also expected to persist in regions of high stress (24), such as during treatment, if cooperative benefits of resistance outweigh the costs of competition for resources (36). Alternatively, facilitation is also expected to be ineffective at low population sizes when cells cannot produce sufficient concentrations of facilitation factor. With these so-called Allee effects (22, 23), cancer populations below a critical abundance cannot generate enough proliferative signals to grow despite the effects of treatment, leading to further reduced facilitation and the population being driven to eradication. Within patient tumors, other regulatory mechanisms, such as cancer-immune interactions may cause more complex forms of frequency or density dependent growth, with diverse growth factors and micro-environmental interactions modifying drug response. Nevertheless, blocking facilitation has clinically valuable features that deserve additional assessment.

Mathematical modeling (57-59) and experimental (26, 60, 61) research proposes that tumor growth and progression may be promoted by cooperation between cells by sharing of resources or products in diverse cell populations. One example involves recruiting the growth of new blood vessels (neoangiogenesis) to supply nutrients and oxygen, as in the case of *ras* oncogene-expressing cancer cells that are capable of down regulating angiogenesis-inhibitory factor thrombospondin-1 production by stromal fibroblasts, promoting an ideal environment for new blood vessel formation benefiting other nearby cells (57). Another example involves growth factor production to drive proliferation, such as the IGF-II provided by insulinoma cells to cells that are not capable of its production (61). Our results support the concept that cancer cell facilitation may impact heterogeneous tumor growth during treatment in ER-positive breast cancer. No current therapy is directed specifically at cooperative cancer cell interactions. However, as tumors are often comprised of multiple different subclonal populations, interactions between cells and their impact on the effectiveness of therapy may provide targets for long-term treatment strategies. Given that facilitation can increase both persistence and biomass relative to simpler systems with resource competition only (24, 62), it is likely to be frequent in heterogeneous cancer populations. As we gain in capabilities to measure the growth of heterogeneous subclone populations during treatment,

we may tailor strategies to control faster growing yet drug sensitive cells while preventing dominance of refractory cells through competition with more fit subclones.

This study is the first to describe facilitation through an increase of local estradiol concentrations by resistant cells, which stimulates proliferation of sensitive cells during selective pressure due to higher dependence on and response to estrogen. It is known that estrogen biosynthesis and metabolism can occur in cancer cells (63-65). It remains unknown how resistant cells in our system acquire the ability to increase estradiol levels. However, the increase of this active estrogen is important given that the majority of breast cancers are hormone receptor positive, and resistance to first line standard of care hormone therapy is common (66-68). In patients with increased levels of local estradiol, potential treatment strategies could include blocking enzymes that synthesize estradiol in resistant cells or modulating the level or type of endocrine therapy given to a patient. Targeting the diffusible facilitation factor has been proposed to be a more evolutionarily stable treatment strategy than targeting the cancer cell receptors or signaling pathways (69) because the production provides little benefit to the producing cell. Understanding and modeling the mechanisms underlying growth and interaction can guide the timing, dosage and targets of therapy for further experimental testing.

In conclusion, our data indicate that the interactions within heterogeneous cancer cell populations shape the dynamics of resistance and cancer growth of the population as a whole. We show that local production of a highly active estrogen, estradiol, facilitates the growth of sensitive cells, is produced by resistant cells, and conveys resistance to anti-proliferative effects of cell cycle inhibition in sensitive cells. We use mathematical models to show that blocking this facilitation mechanism promotes response of the entire cancer population, reducing selection for refractory resistant states. This work provides support for the development of novel cancer therapeutics that include consideration of cooperation within breast cancer.

# Methods

## ***Cell lines and reagents***

The previously authenticated estrogen-receptor-positive (ER+) CAMA-1 and MCF7 breast cancer cell lines were maintained in DMEM+ 10% FBS+ 1% antibiotic–antimycotic solution. Ribociclib-resistant CAMA-1 and MCF7 cell lines were created (ribociclib-resistant CAMA-1 creation previously reported (70)). Briefly, cells were cultured and continuously treated with ribociclib (Selleck Chemicals, Cat. No: S7440) at 1 µM for 1 month for CAMA-1 cells and 7 weeks for MCF7 cells. Following the initial 1 µM ribociclib treatment, CAMA-1 cells were then treated with 250 nM for 4 months while MCF7 cells were treated with 1.5 µM ribociclib for 3 months to develop resistance. Maintenance of ribociclib-resistant CAMA-1 cells continued in complete culture medium + 250 nM ribociclib. Maintenance of ribociclib-resistant MCF7 cells continued in complete culture medium + 1.5 µM ribociclib. Resistance against ribociclib was detected by the

alteration of the dose–response curve measured using CellTiterGlo Chemoluminescent Kit (Promega Corporation, Cat. No.: G7573).

***<u>Lentiviral labeling of sensitive and resistant cells</u>***

Ribociclib resistant lines were evolved under continuous exposure to treatment and with acquired resistance confirmed by dose-response experiments (as described in methods – ***Cell lines and reagents***). Lentiviral labeling of sensitive and resistant cells was previously reported (70). Briefly, using lentiviruses incorporating distinct fluorescent proteins, we labeled parental sensitive cells (venus; LeGO-V2), ribociclib resistant CAMA-1 cells (cerulean; LeGO-Cer2), and ribociclib resistant MCF7 cells (mCherry; LeGO-C2). LeGO-V2, LeGO-Cer2, and LeGO-C2 vectors were provided by Boris Fehse (Addgene plasmids #27340, #27338, and #27339). Lentiviruses with fluorescent proteins were created using Lipofectamine 3000 reagent (Thermo Fisher Scientific) following manufacturer's protocol. CAMA-1 sensitive and resistant cell lines were transduced with lentivirus using reverse transduction. Briefly, 1mL of polybrene-containing cell suspension of 200,000 cells were plated in a well of a 6-well plate. Previously, 0.5 mL of viral aliquot had been dispensed in plate. Following 48 hours of incubation at 37 $^{o}$C with 5% $CO_2$, cells were washed and given fresh regular culture medium. To select for fluorescence-activated cells, fluorescently labeled cells were sorted after further subculture of transduced cells attain homogenously labeled cell populations.

***<u>Mono- and coculture 3D spheroid experiments</u>***

18-21 day-long experiments were initiated with fluorescently labeled sensitive and resistant cell lines in different compositions. For CAMA-1 spheroid experiments, as earlier reported (70), 2000 cells were plated in different proportions (100% CAMA-1 sensitive, 50% CAMA-1 sensitive—50% CAMA-1 resistant, 100% CAMA-1 resistant) in 96-well round-bottom ultra-low attachment spheroid microplate (Corning, Cat. No.: 4520). For MCF7 spheroid experiments, 5000 cells were plated in different proportions (100% MCF7 sensitive, 90% MCF7 sensitive—10% MCF7 resistant, 100% MCF7_resistant) in 96 well microplates as well. 24 h later, spheroids were washed and fresh medium including treatment drugs was applied. Spheroids were treated for a total of 18-21 days with imaging and media change performed at every 4th and 7th day of the week. Spheroids were treated with the following drug therapies at specified doses described in results and figures 1-4: ribociclib (Selleck Chemicals, Cat. No: S7440), estradiol (Peprotech, Cat. No: 5022822), fulvestrant (Selleck Chemicals, Cat. No: S1191), tamoxifen (Selleck Chemicals, Cat. No: S7827), and raloxifene (Selleck Chemicals, Cat. No: S5781). Imaging was performed using Cytation 5 imager (Biotek Instruments) recording signal intensity from brightfield, YFP (for Venus fluorescence) CFP 450/440 (for Cerulean fluorescence) and Texas Red (for mCherry fluorescence) channels. Raw data processing and image analysis were performed using Gen5 3.05 and 3.10 software (Biotek Instruments). Briefly, the stitching of 2 × 2 montage images and Z-projection of 6 layers using focus stacking was performed on raw images followed by spheroid area analysis. To quantify growth under these conditions, we measured fluorescence intensity and growth of

spheroid area over the total time of the experiment. For cell count calculations, a standard curve was created by measuring the area of spheroids after plating at different cell numbers 24 hours after plating. A resulting equation by fitting a curve to the data was performed by GraphPad Prism 7.02 software (second order polynomial – quadratic – curve fit used). Whole spheroid area and fluorescence intensity measurements of each population were integrated into the fitted equation, and cell counts for each population were produced from fluorescence intensities relative to spheroid size. All coculture experiments were performed in triplicates.

***<u>Liquid chromatography-tandem mass spectrometry (LC-MS/MS)</u>***

Media samples taken at day 21 from 3D spheroid experiments, treated with or without ribociclib, (experimental setup previously described in results and methods - ***Mono- and coculture 3D spheroid experiments***) and plated in different compositions (100% sensitive, 50% sensitive – 50% resistant, and 100% resistant) were spun down at 300g and frozen at -80 $^{o}$C. Samples were then prepared by the Analytical Pharmacology Core of City of Hope National Medical Center for LC-MS/MS for estrone and estradiol detection. LC-MS/MS system consisted of a Shimadzu Prominence HPLC system interfaced to an AB SCIEX QTRAP® 5500 system (Foster City, CA, USA). HPLC separation was achieved using a XSELECT CSH Phenyl-Hexyl 3.5um, 2.1x150mm analytical column (Waters™) The column temperature was maintained at 50$^{o}$C, and the flow rate was 0.38ml/min. The mobile phase consisted of A (Water: 1000ml + 60ul 30%NH4OH ) and B (Methanol : 1000ml+ 60ul 30% NH4OH). The following gradient program was used: 55% B (0.01 min), 70% B (0.01-4.0 min), 100% B (5.5min), 30%B (8.5min) The total run time was 8.5min. The auto-injector temperature was maintained at 15 $^{o}$C. The atmospheric pressure chemical ionization (APCI)source of the mass spectrometer was operated in negative ion mode with ion source gas (55), curtain gas (20), collision gas (High), nebulizer current -4.0, The entrance potential was set to -10V. Declustering potential (DP) was -110, collision energy (CE), and collision cell exit potential (CXP) was optimized to -50V, -21V for Estrone, -160V, -50V,-17V for Estrone internal standard), -210V,-58V,-19V for Estradiol and -205V,-52V, -13V for Estradiol internal standard respectively. The source temperature was 400 $^{o}$C. A solvent delay program was used from 0 to 3.5 min and from 6.5 to 8.5min to minimize the mobile phase flow to the source. Analyst software version 1.5.1 was used for data acquisition and processing. Atmospheric – pressure chemical ionization of Estrone, Estrone D4 , Estradiol , Estradiol D5 produced abundant protonated molecular ions (MH-) at m/z 268.980, 272.983, 270.969, and 275.981 respectively. Fragmentation of these compounds was induced under collision induced dissociation conditions. The precursor→product ion combinations at m/z 268.980→145.200 for Estrone, and 272.983→147.100 for Estrone-I.S. 270.969→182.800 and 275.981→147.000 for Estradiol and Estradiol-IS were used in multiple-reaction monitoring mode for quantitation. Under optimized assay conditions, the retention times for Estrone, Estrone IS and Estradiol, Estradiol -IS. were 4.89, 4.60 min, respectively.

***Estradiol production and uptake analysis***

To estimate the production and use of estradiol by sensitive and resistant cells, we compare the fits of three functions, each based on Michaelis-Menten kinetics by minimizing the least squares difference from the observed estradiol concentration. The full model includes separate production and uptake rates for each cell type. We estimate the production parameters $\rho_R$ and $\rho_S$ and the uptake parameters $a_R$ and $a_S$, where $R$ and $S$ represent the measured cell numbers, with the function

$$f_4 = \frac{\rho_R R + \rho_S S}{1 + a_R R + a_S S}$$

We examined simpler models that restrict the values. To test a model without production by sensitive cells, we set $\rho_S = 0$, giving

$$f_3 = \frac{\rho_R R}{1 + a_R R + a_S S}.$$

Because uptake by cells is large compared with background usage (scaled to 1 in each of these models), we tested a simplified model with background usage set to zero. Without that term, the model is overparameterized, and we scale $a_R = 1$. In this case, $a_S$ represents per cell uptake by sensitive cells relative to resistant cells, and the function simplifies to

$$f_2 = \frac{\rho_R R + \rho_S S}{R + a_S S}.$$

In the fits, we eliminate one outlier (Sample F8). We used the reported lower limit of detection of LLOD = 62.5 and set all measured values of 0 to LLOD/2. Neglecting this adjustment leads to significantly worse fits.

Model $f_3$ provided a poor fit. The best fit with model $f_4$ estimates $\rho_R = 83.58$, $\rho_S = 10.11, a_R = 0.864, a_S = 0.345$ and a residual sum of squares of 7321.1. The best fit parameters with model $f_2$ have the same residual sum of squares, with estimates $\rho_R = 96.79, \rho_S = 11.71, a_S = 0.400$. Due to the equally good fit with one fewer parameter, we choose this as our final model.

To find confidence limits, we use the residual sum of squares to estimate the variance and convert the least squares into a likelihood. We find values of each parameter with log likelihood within 2 of the maximum. With model $f_2$, we find limits $\rho_R \in [91.49,102.08], \rho_S \in [9.88,13.54]$, $a_S \in [0.355,0.460]$.

***Mathematical modeling – FACT analysis***

**Facilitation Analysis through Combination Therapy:** The FACT algorithm breaks into six

steps, which we outline here before describing in detail below. Modifiers refer to estrogen pathway modifying treatments, including estradiol itself and three ER antagonists: fulvestrant, tamoxifen, and raloxifene.

1. **Fit growth and carrying capacity** for each cell type in monoculture with no treatment.
2. **Treatment effects:** Using the carrying capacity in the absence of treatment, find the effects of ribociclib or modifier treatment on cell growth and death rates.
3. **Synergy:** From growth with combined ribociclib and modifier treatment, compare observed growth with that expected under a null model without interaction.
4. **Competition coefficients:** Using the carrying capacities and growth in sensitive and resistant cells in monoculture from Step 1, estimate competition coefficients between the two cell types in coculture.
5. **Facilitation:** Using the carrying capacities, growth and death rates of single cell types with or without ribociclib from Steps 1 and 2, and the competition coefficients in the absence of treatment from Step 3, quantify facilitation as deviations of growth from predicted under a null model. To quantify facilitation in the presence of modifier we follow the same steps but with modifier treatment.
6. **Facilitation modification:** Using the growth of cells in competition with ribociclib (Step 5) and the direct effects of modifier (Step 2), quantify whether the modifier enhances or reduces facilitation.

**Detailed mathematical methods**

We fit each model with least squares, using all three replicates and the observed mean on day 4 for the initial condition. We exclude the measurements before day 4 because the cells often show a lag before beginning their growth.

**1. Fit growth and carrying capacity to single cell data in the absence of treatment.** We use the logistic model, as defined by the differential equations for sensitive and resistant cells

$$\frac{dS}{dt} = r_S\left(1 - \frac{S}{K_S}\right)$$

$$\frac{dR}{dt} = r_R(1 - \frac{R}{K_R})$$

to estimate $r_S$, $r_R$, $K_S$ and $K_R$ as the growth rates and carrying capacities of sensitive (S) cells and resistant (R ) cells.

**2. Treatment and modifier effects:** Using the carrying capacity in the absence of treatment we estimate growth with treatment ($r_{ST}$ , $r_{RT}$) as shown, and with modifier ($r_{SM}$ , $r_{RM}$) with the model

$$\frac{dS}{dt} = r_{ST}\left(1 - \frac{S}{K_S}\right)$$

$$\frac{dR}{dt} = r_{RT}\left(1 - \frac{R}{K_R}\right)$$

**3. Synergy**: To quantify how ribociclib interacts with modifiers in monoculture, we fit the logistic model using carrying capacities from Step 1, and compare the estimated growth $r_c$ with the null

model

$$r_S\left(\frac{r_{ST}}{r_S}\right)\left(\frac{r_{SM}}{r_S}\right)$$

**4. Estimate competition coefficients:** Using the estimates of the growth rates and carrying capacities from Step 1, we fit untreated coculture data to a Lotka-Volterra competition model with competition coefficients $\alpha_{SR}$ and $\alpha_{RS}$

$$\frac{dS}{dt} = r_S\left(1 - \frac{S + \alpha_{SR}R}{K_S}\right)$$

$$\frac{dR}{dt} = r_R\left(1 - \frac{\alpha_{RS}S + R}{K_S}\right)$$

**5. Estimate facilitation:** We estimate facilitation as the deviation between observed and expected growth. To find expected growth, we use the estimates of the growth rates in monoculture with treatment, carrying capacities from the untreated monoculture, and the competition coefficients from the untreated cocultures.

**6. Facilitation modification:** If the presence of the other cell type enhances growth in the presence of ribociclib, a modifier could cancel or enhance this effect. To quantify, we use the growth parameter from step 4 in the presence of ribociclib, and account for the direct effects of the modifier as in step 2.

***<u>Facilitation Analysis by Combination Therapy – Mechanistic model:</u>***

**Facilitation factor production, flux and utilization**

To describe the mechanisms of facilitation between resistant (R) and sensitive (S) cells, we model the intracellular concentration of the facilitation factor (E) in each cell type ($E_S, E_R$) , and the flux of this factor between cell types via the shared extra-cellular environment ($E_E$). We describe the intracellular production of this factor by sensitive and resistant cells at rate $\rho_S$ and $\rho_R$ and the receptor binding for utilization as a growth promoting signal at rate $\mu_S$ and $\mu_R$. Facilitation factors diffuse between cells types and the extra-cellular environment at rate $\eta$. Finally, we describe the influx ($\sigma_E$) and decay ($\delta_E$) of facilitation factors from the external environment. This leads to the following set of differential equations describing cellular and environmental concentrations of facilitation factors:

$$\frac{dE_S}{dt} = \rho_S + \eta(E_E - E_S) - \mu_S E_S$$

$$\frac{dE_R}{dt} = \rho_R + \eta(E_E - E_R) - \mu_R E_R$$

$$\frac{dE_E}{dt} = \sigma_E + \eta(E_S - E_E) + \eta(E_R - E_E) - \delta_E E_E.$$

The equilibrium of this system is:

$$E_E^* = \frac{\sigma_E + \rho_S S \frac{\eta}{\eta + \mu_S} + \rho_R R \frac{\eta}{\eta + \mu_R}}{\eta S \frac{\mu_S}{\eta + \mu_S} + \eta R \frac{\mu_R}{\eta + \mu_R} + \delta_E}$$

$$E_S = \frac{\rho_S + \eta E_E^*}{\eta + \mu_S}$$

$$E_R = \frac{\rho_R + \eta E_E^*}{\eta + \mu_R},$$

showing that the intra- and extracellular concentrations depend on the net balance between sources and sinks of facilitation factors. Inhibitors of the production of facilitation factors will reduce the intra and extracellular inputs to E ($\sigma$ and $\rho$). In contrast drugs targeting facilitation factor receptors will reduce the binding of intracellular factors, reducing $\mu$ by some factor.

**Coupling facilitation factor dynamics with cancer coculture spheroid growth**

The cellular level description of facilitation was next scaled to describe the populations of resistant and sensitive cells competing and facilitating in coculture spheroids over time. The resistant and sensitive cells are described as transitioning between proliferative (P), quiescent (Z) and senescent (X) states.

Resource competition between all cells is described by the following term:

$$\alpha(P, Z, X) = 1 - \sum_{i=1}^{n} \frac{P_i + Z_i + X_i}{K_i},$$

where competitive ability of each cell type (i) is determined by the carrying capacity parameter $K_i$.

Proliferative cells enter the G1/S phase cell cycle checkpoint at a baseline rate (r), which is reduced by resource competition and increased by facilitation factor availability (E). This beneficial facilitation factor effect saturates at high concentrations when uptake and binding becomes rate limited (c). The proliferation rate of resistant and sensitive cells will be related to the binding of intracellularly available facilitation factors ($\mu_i E_i$). The G1/S phase entry of cells of type i, based on competition and the internal concentration of facilitation factors therefore follows:

$$G_i = r_i\left(1 + \frac{\mu_i E_i}{1 + c\mu_i E_i}\right)\alpha(P, Z, X)$$

After entering the cell cycle checkpoint, cells undertake the decision to divide or enter a quiescent state, based on the balance of key regulatory cell cycle promoters and inhibitors. In addition to a

baseline quiescence rate ($\lambda_i$), cells are promoted to enter the quiescent state by the cell cycle inhibitor ribociclib (x), which inactivates the key regulators of the G1/S phase cell cycle checkpoint (CDK4/6), blocking cell cycle progression. We describe the effect of ribociclib in inhibiting cell cycle progression and driving cells into a quiescent state as increasing with drug concentration following:

$$q_i(x) = \frac{x}{k_i + x}.$$

No additional quiescence is induced in the absence of treatment, complete cell cycle arrest is achieved at very high levels of ribociclib and the half maximal cell cycle arrest is achieved at a dose $k_i$for cell type i. Differences in this parameter between resistant and sensitive cells describes innate resistance to the drug that emerged through selection. Following quiescence, we describe the transition of cells into a senescent state at rate $\varphi_i$ before cell death occurs at rate $\delta_i$.

Combining these models of competition, facilitation, cell cycle progression, arrest and cell death yields the following spheroid population model, describing the abundance of proliferative quiescent and senescent resistant and sensitive cells in coculture spheroids over time. The dynamics of the extracellular facilitation factor concentration in the spheroid population model is governed by the balance between net secretion by proliferative and quiescent cells (resistant= $\gamma_R$ and sensitive= $\gamma_S$) and its decay ($\delta_E$), giving:

$$\frac{dP_i}{dt} = (G_i(1 - q_i(x)) - G_i q_i(x) - \lambda_i)P_i$$

$$\frac{dZ_i}{dt} = (G_i q_i(x) - \lambda_i)P_i - \varphi_i Z_i$$

$$\frac{dX_i}{dt} = \varphi_i Z_i - \delta_i X_i$$

$$\frac{dE_E}{dt} = \left(\sum \gamma_i (P_i + Z_i)\right) - \delta_E E_E.$$

**Resistant and sensitive cell coculture spheroid growth and facilitation across drug doses**

Resistant and sensitive cells were fluorescently labeled as previously described in methods (***Lentiviral labeling of sensitive and resistant cells***) and replicate populations (n=3) were plated either in monoculture or in 50:50 initial coculture. Cancer spheroids were grown in 3D culture for 21 days with imaging performed at 3-4 day intervals and the abundance of each cell type enumerated as described previously in methods (***Mono- and coculture spheroid experiments*****).** To explore the consequence of cell-cell interactions of drug response, the replicated mono- and coculture time course experiments were conducted under 8 ribociclib concentrations within the EC20-50 range (0,100,200,400,600,800,1000,2000nM). Spheroid analysis and cell counts performed as described previously in methods (***Mono- and coculture spheroid experiments*****)**

## Measuring the strength of competitive and facilitative interactions between subclones and vital cellular rates

We measured the strength of competitive and facilitative interactions between subclones, the drug impacts on cell cycle arrest and the vital cellular rates of proliferation, quiescence and senescence, by fitting the spheroid population model to the experimental data described above. Given the initial spheroid size and composition and the ribociclib concentration, the spheroid population model projects the abundance of sensitive and resistant cells throughout the experiment based on a given combination of biological rates. A log normal distribution measurement model was used to evaluate the likelihood of each spheroid abundance observation and weakly informative priors were used in all cases (Supplementary methods). The biological rates of each process in the spheroid population model were inferred with uncertainty, using Bayesian Hamiltonian Monte Carlo (HMC) (71). Biological rates were identified that yield the most accurate model predictions of the observed spheroid growth trajectories and composition over time and across all drug doses. The HMC algorithm efficiently samples the posterior distribution, describing the likely biological rates given the model, using derivatives of the probability density function. As a result, the inference approach jointly and efficiently: i) identifies the most probable range of subclone interaction strengths (competition and facilitation), ii) predicts the cellular composition and facilitation factor concentration throughout the experiments and iii) provides a probabilistic measurement of the likelihood of the hypothesis encoded by the model given the available data.

## Comparing alternative hypotheses (models) of the mechanisms generating spheroid growth

We assessed the support for the hypothesis that facilitation is playing an important role in influencing the growth of spheroids containing resistant and sensitive cells. We generated a range of alternative hypotheses about processes that could generate the spheroid growth dynamics and formally compared the performance of these models at explaining the data, after each was fitted to the data (as described above). Specifically, we developed alternative population level models hypothesizing that the spheroid growth trajectories and composition were driven by:

a) Competition alone: Resistant and sensitive cells have differing proliferation and death rates and compete. These aspects are included in each of the extensions.
b) Plasticity (DI): Drug induced phenotypic plasticity inducing a transition of both cell types to a more resistant state.
c) Plasticity (RS): Random phenotypic switching of both cell types between a more and less susceptible state.
d) Facilitation Symmetric (1-State): Facilitation of equal strength between resistant and sensitive (Allee effect model).
e) Facilitation (1-State): Facilitation where resistant and sensitive cells contribute differently to the production of a growth promoting signal.
f) Facilitation (2-State): Facilitation where resistant and sensitive cells contribute differently to the production of a growth promoting signal and ribociclib treatment induces senescence.
g) Facilitation (3-State) (the full model): Facilitation where resistant and sensitive cells contribute differently to the production of a growth promoting signal and ribociclib treatment induces quiescence and then senescence.

The support for each hypothesis was measured by calculating the penalized prediction error of each model, using WAIC (widely applicable information criterion) to avoiding overfitting the data by penalizing the model likelihood based on model complexity (52).

**Model predictions of final spheroid size when modulating the strength of facilitation**

To explore the consequences of blocking facilitation, we analyzed the impact on resistant and sensitive cell abundances of reducing the rate of receptor binding with facilitation factors. The most likely values of the receptor binding parameters of each cell type ($\mu_S$ and $\mu_R$) were reduced by a factor $\zeta$ (between 0 and 80% reduction). Using the model and holding all other parameters constant, the predicted abundance of sensitive and resistant cells after 21 days of coculture was forecasted, assuming continuous facilitation blocking throughout this period.

807

808

809 ***References:***


810 1. McGranahan N, Swanton C. Clonal Heterogeneity and Tumor Evolution: Past, Present, and the
811 Future. Cell. 2017;168(4):613-28. doi: 10.1016/j.cell.2017.01.018. PubMed PMID: 28187284.
812 2. Delou JMA, Souza ASO, Souza LCM, Borges HL. Highlights in Resistance Mechanism Pathways for
813 Combination Therapy. Cells. 2019;8(9). doi: 10.3390/cells8091013. PubMed PMID: 31480389; PubMed
814 Central PMCID: PMC6770082.
815 3. Fedele C, Tothill RW, McArthur GA. Navigating the challenge of tumor heterogeneity in cancer
816 therapy. Cancer discovery. 2014;4(2):146-8. doi: 10.1158/2159-8290.CD-13-1042. PubMed PMID:
817 24501303.
818 4. Swanton C. Intratumor heterogeneity: evolution through space and time. Cancer research.
819 2012;72(19):4875-82. doi: 10.1158/0008-5472.CAN-12-2217. PubMed PMID: 23002210; PubMed Central
820 PMCID: PMC3712191.
821 5. Brady SW, McQuerry JA, Qiao Y, Piccolo SR, Shrestha G, Jenkins DF, et al. Combating subclonal
822 evolution of resistant cancer phenotypes. Nature communications. 2017;8(1):1231. doi: 10.1038/s41467-
823 017-01174-3. PubMed PMID: 29093439; PubMed Central PMCID: PMC5666005.
824 6. Beckman RA, Loeb LA. Evolutionary dynamics and significance of multiple subclonal mutations in
825 cancer. DNA repair. 2017;56:7-15. doi: 10.1016/j.dnarep.2017.06.002. PubMed PMID: 28652129;
826 PubMed Central PMCID: PMC5551892.
827 7. Kim C, Gao R, Sei E, Brandt R, Hartman J, Hatschek T, et al. Chemoresistance Evolution in Triple-
828 Negative Breast Cancer Delineated by Single-Cell Sequencing. Cell. 2018;173(4):879-93 e13. doi:
829 10.1016/j.cell.2018.03.041. PubMed PMID: 29681456; PubMed Central PMCID: PMC6132060.
830 8. Gluckman PD, Low FM, Buklijas T, Hanson MA, Beedle AS. How evolutionary principles improve
831 the understanding of human health and disease. Evol Appl. 2011;4(2):249-63. doi: 10.1111/j.1752-
832 4571.2010.00164.x. PubMed PMID: WOS:000287451800007.
833 9. Gatenby RA, Vincent TL. Application of quantitative models from population biology and
834 evolutionary game theory to tumor therapeutic strategies. Molecular cancer therapeutics. 2003;2(9):919-
835 27. PubMed PMID: 14555711.
836 10. Sieber OM, Tomlinson SR, Tomlinson IP. Tissue, cell and stage specificity of (epi)mutations in
837 cancers. Nature reviews Cancer. 2005;5(8):649-55. doi: 10.1038/nrc1674. PubMed PMID: 16056260.
838 11. Crespi B, Summers K. Evolutionary biology of cancer. Trends in ecology & evolution.
839 2005;20(10):545-52. doi: 10.1016/j.tree.2005.07.007. PubMed PMID: 16701433.
840 12. Pienta KJ, McGregor N, Axelrod R, Axelrod DE. Ecological therapy for cancer: defining tumors using
841 an ecosystem paradigm suggests new opportunities for novel cancer treatments. Translational oncology.
842 2008;1(4):158-64. doi: 10.1593/tlo.08178. PubMed PMID: 19043526; PubMed Central PMCID:
843 PMC2582164.
844 13. Heppner GH. Cancer cell societies and tumor progression. Stem cells. 1993;11(3):199-203. doi:
845 10.1002/stem.5530110306. PubMed PMID: 8318906.
846 14. Gatenby RA, Brown JS. The Evolution and Ecology of Resistance in Cancer Therapy. Cold Spring
847 Harbor perspectives in medicine. 2020;10(11). doi: 10.1101/cshperspect.a040972. PubMed PMID:
848 33139405; PubMed Central PMCID: PMC7605238.
849 15. Franco OE, Tyson DR, Konvinse KC, Udyavar AR, Estrada L, Quaranta V, et al. Altered TGF-
850 alpha/beta signaling drives cooperation between breast cancer cell populations. FASEB journal : official
851 publication of the Federation of American Societies for Experimental Biology. 2016;30(10):3441-52. doi:
852 10.1096/fj.201500187RR. PubMed PMID: 27383183; PubMed Central PMCID: PMC5024699.

16. Adler FR, Gordon DM. Cancer Ecology and Evolution: Positive interactions and system vulnerability. Current opinion in systems biology. 2019;17:1-7. doi: 10.1016/j.coisb.2019.09.001. PubMed PMID: 32318644; PubMed Central PMCID: PMC7172748.

17. Bhang HE, Ruddy DA, Krishnamurthy Radhakrishna V, Caushi JX, Zhao R, Hims MM, et al. Studying clonal dynamics in response to cancer therapy using high-complexity barcoding. Nature medicine. 2015;21(5):440-8. doi: 10.1038/nm.3841. PubMed PMID: 25849130.

18. Martin-Pardillos A, Valls Chiva A, Bande Vargas G, Hurtado Blanco P, Pineiro Cid R, Guijarro PJ, et al. The role of clonal communication and heterogeneity in breast cancer. BMC cancer. 2019;19(1):666. doi: 10.1186/s12885-019-5883-y. PubMed PMID: 31277602; PubMed Central PMCID: PMC6612119.

19. Bowling S, Lawlor K, Rodriguez TA. Cell competition: the winners and losers of fitness selection. Development. 2019;146(13). doi: 10.1242/dev.167486. PubMed PMID: 31278123.

20. Madan E, Peixoto ML, Dimitrion P, Eubank TD, Yekelchyk M, Talukdar S, et al. Cell Competition Boosts Clonal Evolution and Hypoxic Selection in Cancer. Trends in cell biology. 2020;30(12):967-78. doi: 10.1016/j.tcb.2020.10.002. PubMed PMID: 33160818.

21. Zhou H, Neelakantan D, Ford HL. Clonal cooperativity in heterogenous cancers. Seminars in cell & developmental biology. 2017;64:79-89. doi: 10.1016/j.semcdb.2016.08.028. PubMed PMID: 27582427; PubMed Central PMCID: PMC5330947.

22. Kanarek AR, Webb CT. Allee effects, adaptive evolution, and invasion success. Evol Appl. 2010;3(2):122-35. doi: 10.1111/j.1752-4571.2009.00112.x. PubMed PMID: 25567913; PubMed Central PMCID: PMC3352477.

23. Vazquez DP, Ramos-Jiliberto R, Urbani P, Valdovinos FS. A conceptual framework for studying the strength of plant-animal mutualistic interactions. Ecology letters. 2015;18(4):385-400. doi: 10.1111/ele.12411. PubMed PMID: 25735791.

24. Bertness MD, Callaway R. Positive interactions in communities. Trends in ecology & evolution. 1994;9(5):191-3. doi: 10.1016/0169-5347(94)90088-4. PubMed PMID: 21236818.

25. Axelrod R, Axelrod DE, Pienta KJ. Evolution of cooperation among tumor cells. Proceedings of the National Academy of Sciences of the United States of America. 2006;103(36):13474-9. doi: 10.1073/pnas.0606053103. PubMed PMID: 16938860; PubMed Central PMCID: PMC1557388.

26. Cleary AS, Leonard TL, Gestl SA, Gunther EJ. Tumour cell heterogeneity maintained by cooperating subclones in Wnt-driven mammary cancers. Nature. 2014;508(7494):113-7. doi: 10.1038/nature13187. PubMed PMID: 24695311; PubMed Central PMCID: PMC4050741.

27. Maley CC, Aktipis A, Graham TA, Sottoriva A, Boddy AM, Janiszewska M, et al. Classifying the evolutionary and ecological features of neoplasms. Nature reviews Cancer. 2017;17(10):605-19. doi: 10.1038/nrc.2017.69. PubMed PMID: 28912577; PubMed Central PMCID: PMC5811185.

28. Archetti M. Cooperation between cancer cells. Evolution, medicine, and public health. 2018;2018(1):1. doi: 10.1093/emph/eoy003. PubMed PMID: 29410785; PubMed Central PMCID: PMC5793724.

29. Oates K, Wilson M. Nominal kinship cues facilitate altruism. Proceedings Biological sciences. 2002;269(1487):105-9. doi: 10.1098/rspb.2001.1875. PubMed PMID: 11798424; PubMed Central PMCID: PMC1690876.

30. Wilson DS, Pollock GB, Dugatkin LA. Can Altruism Evolve in Purely Viscous Populations. Evol Ecol. 1992;6(4):331-41. doi: Doi 10.1007/Bf02270969. PubMed PMID: WOS:A1992JD08100005.

31. Bruno JF, Stachowicz JJ, Bertness MD. Inclusion of facilitation into ecological theory. Trends in ecology & evolution. 2003;18(3):119-25. doi: Pii S0169-5347(02)00045-9

Doi 10.1016/S0169-5347(02)00045-9. PubMed PMID: WOS:000181729900007.

898 32. Caldwell MM, Dawson TE, Richards JH. Hydraulic lift: Consequences of water efflux from the roots
899 of plants. Oecologia. 1998;113(2):151-61. doi: DOI 10.1007/s004420050363. PubMed PMID:
900 WOS:000071658500001.
901 33. de Mazancourt C, Schwartz MW. A resource ratio theory of cooperation. Ecology letters.
902 2010;13(3):349-59. doi: 10.1111/j.1461-0248.2009.01431.x. PubMed PMID: 20455920.
903 34. Leigh EG, Jr. The evolution of mutualism. Journal of evolutionary biology. 2010;23(12):2507-28.
904 doi: 10.1111/j.1420-9101.2010.02114.x. PubMed PMID: 20942825.
905 35. Tabassum DP, Polyak K. Tumorigenesis: it takes a village. Nature reviews Cancer. 2015;15(8):473-
906 83. doi: 10.1038/nrc3971. PubMed PMID: 26156638.
907 36. Travis JM, Brooker RW, Dytham C. The interplay of positive and negative species interactions
908 across an environmental gradient: insights from an individual-based simulation model. Biology letters.
909 2005;1(1):5-8. doi: 10.1098/rsbl.2004.0236. PubMed PMID: 17148114; PubMed Central PMCID:
910 PMC1629044.
911 37. Deisboeck TS, Couzin ID. Collective behavior in cancer cell populations. Bioessays. 2009;31(2):190-
912 7. doi: 10.1002/bies.200800084. PubMed PMID: WOS:000263863600009.
913 38. Azuma K, Kawahara A, Sonoda K, Nakashima K, Tashiro K, Watari K, et al. FGFR1 activation is an
914 escape mechanism in human lung cancer cells resistant to afatinib, a pan-EGFR family kinase inhibitor.
915 Oncotarget. 2014;5(15):5908-19. doi: 10.18632/oncotarget.1866. PubMed PMID: 25115383; PubMed
916 Central PMCID: PMC4171601.
917 39. Rozeboom B, Dey N, De P. ER+ metastatic breast cancer: past, present, and a prescription for an
918 apoptosis-targeted future. American journal of cancer research. 2019;9(12):2821-31. PubMed PMID:
919 31911865; PubMed Central PMCID: PMC6943351.
920 40. Harvey JM, Clark GM, Osborne CK, Allred DC. Estrogen receptor status by immunohistochemistry
921 is superior to the ligand-binding assay for predicting response to adjuvant endocrine therapy in breast
922 cancer. J Clin Oncol. 1999;17(5):1474-81. doi: Doi 10.1200/Jco.1999.17.5.1474. PubMed PMID:
923 WOS:000080267900020.
924 41. Rani A, Stebbing J, Giamas G, Murphy J. Endocrine Resistance in Hormone Receptor Positive
925 Breast Cancer-From Mechanism to Therapy. Front Endocrinol (Lausanne). 2019;10:245. Epub 2019/06/11.
926 doi: 10.3389/fendo.2019.00245. PubMed PMID: 31178825; PubMed Central PMCID: PMCPMC6543000.
927 42. Zhao H, Zhou L, Shangguan AJ, Bulun SE. Aromatase expression and regulation in breast and
928 endometrial cancer. J Mol Endocrinol. 2016;57(1):R19-33. Epub 2016/04/14. doi: 10.1530/jme-15-0310.
929 PubMed PMID: 27067638; PubMed Central PMCID: PMCPMC5519084.
930 43. Osborne CK. Tamoxifen in the treatment of breast cancer. N Engl J Med. 1998;339(22):1609-18.
931 Epub 1998/11/26. doi: 10.1056/nejm199811263392207. PubMed PMID: 9828250.
932 44. Effects of chemotherapy and hormonal therapy for early breast cancer on recurrence and 15-year
933 survival: an overview of the randomised trials. Lancet. 2005;365(9472):1687-717. Epub 2005/05/17. doi:
934 10.1016/s0140-6736(05)66544-0. PubMed PMID: 15894097.
935 45. Company ELa. Endocrine Therapy With or Without Abemaciclib (LY2835219) Following Surgery in
936 Participants With Breast Cancer (monarchE) 2017 [updated September 18, 2020; cited 2020 October 13].
937 Available from: https://www.clinicaltrials.gov/ct2/show/NCT03155997.
938 46. Pharmaceuticals N. A Trial to Evaluate Efficacy and Safety of Ribociclib With Endocrine Therapy as
939 Adjuvant Treatment in Patients With HR+/HER2- Early Breast Cancer (NATALEE) 2018 [updated October
940 2, 2020; cited 2020 October 13]. Available from: https://clinicaltrials.gov/ct2/show/NCT03701334.
941 47. Bertagnolli M ME, DeMichele A, Gnant M. PALbociclib CoLlaborative Adjuvant Study (PALLAS)
942 2015 [updated March 9, 2020; cited 2020 October 2013]. Available from:
943 https://clinicaltrials.gov/ct2/show/NCT02513394.
944 48. PENELOPE-B TRIAL OF IBRANCE® (PALBOCICLIB) IN EARLY BREAST CANCER DID NOT MEET
945 PRIMARY ENDPOINT: Pfizer; 2020 [updated October 9, 2020; cited 2020 October 13]. Available from:

946 https://www.pfizer.com/news/press-release/press-release-detail/penelope-b-trial-ibrancer-palbociclib-
947 early-breast-cancer.
948 49. Johnston S, Puhalla S, Wheatley D, Ring A, Barry P, Holcombe C, et al. Randomized Phase II Study
949 Evaluating Palbociclib in Addition to Letrozole as Neoadjuvant Therapy in Estrogen Receptor-Positive Early
950 Breast Cancer: PALLET Trial. J Clin Oncol. 2019;37(3):178-89. Epub 2018/12/14. doi:
951 10.1200/jco.18.01624. PubMed PMID: 30523750.
952 50. Johnston SRD, Harbeck N, Hegg R, Toi M, Martin M, Shao ZM, et al. Abemaciclib Combined With
953 Endocrine Therapy for the Adjuvant Treatment of HR+, HER2-, Node-Positive, High-Risk, Early Breast
954 Cancer (monarchE). J Clin Oncol. 2020;38(34):3987-98. Epub 2020/09/22. doi: 10.1200/jco.20.02514.
955 PubMed PMID: 32954927; PubMed Central PMCID: PMCPMC7768339.
956 51. Flack JC, Girvan M, de Waal FB, Krakauer DC. Policing stabilizes construction of social niches in
957 primates. Nature. 2006;439(7075):426-9. doi: 10.1038/nature04326. PubMed PMID: 16437106.
958 52. Resat H, Petzold L, Pettigrew MF. Kinetic modeling of biological systems. Methods in molecular
959 biology. 2009;541:311-35. doi: 10.1007/978-1-59745-243-4_14. PubMed PMID: 19381542; PubMed
960 Central PMCID: PMC2877599.
961 53. Zele F, Magalhaes S, Kefi S, Duncan AB. Ecology and evolution of facilitation among symbionts.
962 Nature communications. 2018;9(1):4869. doi: 10.1038/s41467-018-06779-w. PubMed PMID: 30451829;
963 PubMed Central PMCID: PMC6242936.
964 54. Krakauer DC, Page KM, Erwin DH. Diversity, dilemmas, and monopolies of niche construction. The
965 American naturalist. 2009;173(1):26-40. doi: 10.1086/593707. PubMed PMID: 19061421.
966 55. Holland JN, DeAngelis DL. A consumer-resource approach to the density-dependent population
967 dynamics of mutualism. Ecology. 2010;91(5):1286-95. doi: 10.1890/09-1163.1. PubMed PMID: 20503862.
968 56. Burt FN, Krakauer J, van der Schalie N. Construction of clinical algorithms. Jama.
969 1983;250(18):2471. doi: 10.1001/jama.1983.03340180033017. PubMed PMID: 6688833.
970 57. Kalas W, Yu JL, Milsom C, Rosenfeld J, Benezra R, Bornstein P, et al. Oncogenes and Angiogenesis:
971 down-regulation of thrombospondin-1 in normal fibroblasts exposed to factors from cancer cells
972 harboring mutant ras. Cancer research. 2005;65(19):8878-86. doi: 10.1158/0008-5472.CAN-05-1479.
973 PubMed PMID: 16204059.
974 58. Hanahan D, Folkman J. Patterns and Emerging Mechanisms of the Angiogenic Switch during
975 Tumorigenesis. Cell. 1996;86(3):353-64. doi: https://doi.org/10.1016/S0092-8674(00)80108-7.
976 59. Archetti M, Pienta KJ. Cooperation among cancer cells: applying game theory to cancer. Nat Rev
977 Cancer. 2019;19(2):110-7. Epub 2018/11/25. doi: 10.1038/s41568-018-0083-7. PubMed PMID: 30470829.
978 60. Naffar-Abu Amara S, Kuiken HJ, Selfors LM, Butler T, Leung ML, Leung CT, et al. Transient
979 commensal clonal interactions can drive tumor metastasis. Nature communications. 2020;11(1):5799.
980 doi: 10.1038/s41467-020-19584-1. PubMed PMID: 33199705; PubMed Central PMCID: PMC7669858.
981 61. Archetti M, Ferraro DA, Christofori G. Heterogeneity for IGF-II production maintained by public
982 goods dynamics in neuroendocrine pancreatic cancer. Proceedings of the National Academy of Sciences
983 of the United States of America. 2015;112(6):1833-8. doi: 10.1073/pnas.1414653112. PubMed PMID:
984 25624490; PubMed Central PMCID: PMC4330744.
985 62. Kefi S, van Baalen M, Rietkerk M, Loreau M. Evolution of local facilitation in arid ecosystems. The
986 American naturalist. 2008;172(1):E1-17. doi: 10.1086/588066. PubMed PMID: 18554137.
987 63. Simigdala N, Gao Q, Pancholi S, Roberg-Larsen H, Zvelebil M, Ribas R, et al. Cholesterol
988 biosynthesis pathway as a novel mechanism of resistance to estrogen deprivation in estrogen receptor-
989 positive breast cancer. Breast Cancer Research. 2016;18(1):58. doi: 10.1186/s13058-016-0713-5.
990 64. Harada N. Aberrant expression of aromatase in breast cancer tissues. J Steroid Biochem Mol Biol.
991 1997;61(3-6):175-84. Epub 1997/04/01. PubMed PMID: 9365188.

65. Forbes NS, Meadows AL, Clark DS, Blanch HW. Estradiol stimulates the biosynthetic pathways of breast cancer cells: detection by metabolic flux analysis. Metabolic engineering. 2006;8(6):639-52. doi: 10.1016/j.ymben.2006.06.005. PubMed PMID: 16904360.
66. Pigeault R, Vezilier J, Cornet S, Zele F, Nicot A, Perret P, et al. Avian malaria: a new lease of life for an old experimental model to study the evolutionary ecology of Plasmodium. Philosophical transactions of the Royal Society of London Series B, Biological sciences. 2015;370(1675). doi: 10.1098/rstb.2014.0300. PubMed PMID: 26150666; PubMed Central PMCID: PMC4528498.
67. AlFakeeh A, Brezden-Masley C. Overcoming endocrine resistance in hormone receptor-positive breast cancer. Curr Oncol. 2018;25(Suppl 1):S18-s27. Epub 2018/06/19. doi: 10.3747/co.25.3752. PubMed PMID: 29910644; PubMed Central PMCID: PMCPMC6001756.
68. Gonzalez-Angulo AM, Morales-Vasquez F, Hortobagyi GN. Overview of resistance to systemic therapy in patients with breast cancer. Adv Exp Med Biol. 2007;608:1-22. Epub 2007/11/13. doi: 10.1007/978-0-387-74039-3_1. PubMed PMID: 17993229.
69. Pepper JW. Drugs that target pathogen public goods are robust against evolved drug resistance. Evol Appl. 2012;5(7):757-61. doi: 10.1111/j.1752-4571.2012.00254.x. PubMed PMID: 23144661; PubMed Central PMCID: PMC3492900.
70. Grolmusz VK, Chen J, Emond R, Cosgrove PA, Pflieger L, Nath A, et al. Exploiting collateral sensitivity controls growth of mixed culture of sensitive and resistant cells and decreases selection for resistant cells in a cell line model. Cancer cell international. 2020;20:253. doi: 10.1186/s12935-020-01337-1. PubMed PMID: 32565737; PubMed Central PMCID: PMC7301982.
71. Carpenter B, Gelman A, Hoffman MD, Lee D, Goodrich B, Betancourt M, et al. Stan: a probabilistic programming language. Grantee Submission. 2017;76(1):1-32.

## Acknowledgements

The authors would like to acknowledge the professional support of the Analytical Pharmacology Core of City of Hope National Medical Center, led by Dr. Tim Synold. The authors also thank Dr. Adam Cohen, Dr. Benjamin Decato, Dr. Jeffrey Chang, Dr. Aritro Nath, Dr. Phillip Moos, and Patrick Cosgrove for their comments on the manuscript. This research and JIG, RSS, FRA, and AHB have been supported by an NIH NCI U54CA209978 grant from the National Cancer Institute.

## Author contributions

RE carried out experiments, was involved in their analysis and wrote the manuscript. JIG and FRA carried out the mathematical modeling and facilitation analysis and wrote the manuscript. VKG generated cell lines, performed experiments, and developed system for growth measurements. AHB conceived the study, was involved in data analysis, and wrote the manuscript. RS developed the preliminary mathematical models. All authors approved the final version of the manuscript.

## Competing interests

The authors declare no competing interests.

## Data availability

All data on which results and conclusions are provided as supplemental data with this manuscript.

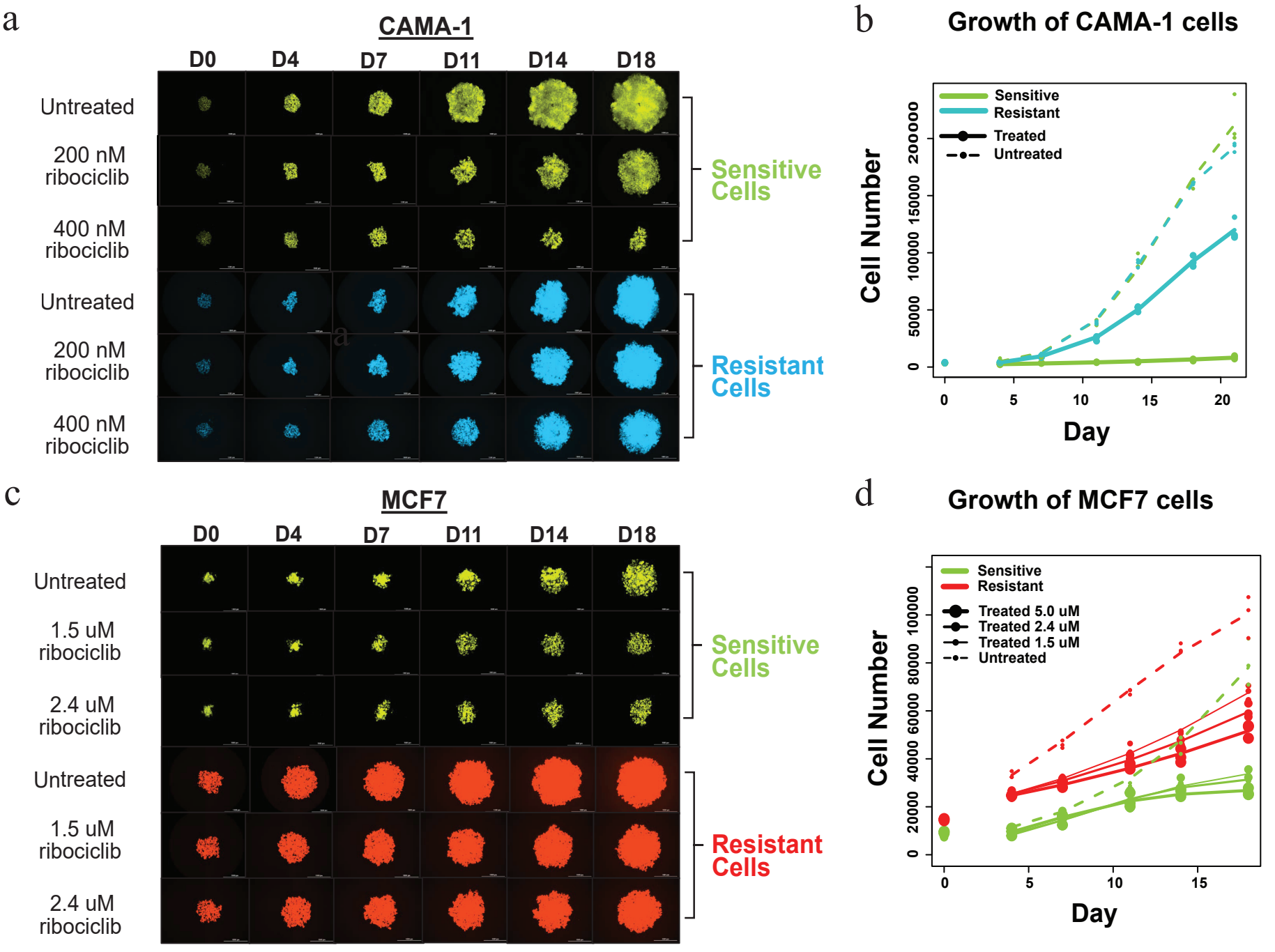


***Figure 1.*** **Sensitive and resistant cell growth and treatment effects. a**, CAMA-1 spheroids of 100% monoculture sensitive (venus, green) or resistant cells (cerulean, blue) cultured in untreated control, 200 nM ribociclib, and 400nM ribociclib treated medium for 18 days. Images taken at Day 18. **b**, Growth curves of CAMA-1 untreated and ribociclib treated sensitive and resistant cell populations; Box plot of CAMA-1 growth of untreated and ribociclib treated sensitive or resistant cells from day 0 to day 14 ($p < 0.0001$ for interaction between cell type and treatment with a linear model) **c**, MCF7 spheroids of 100% monoculture sensitive (venus, green) or resistant cells (mcherry, red) cultured in untreated, 1.5 uM ribociclib, and 2.4 uM ribociclib treated medium for 18 days. Images taken at Day 18. **d**, Growth curves of MCF7 untreated and ribociclib treated sensitive and resistant cell populations ($p < 0.005$ for greater reduction in growth in sensitive cells at each level of treatment based on the interaction term from a linear model of log growth between day 4 and day 18, no significant difference in log growth between day 4 and day 14).

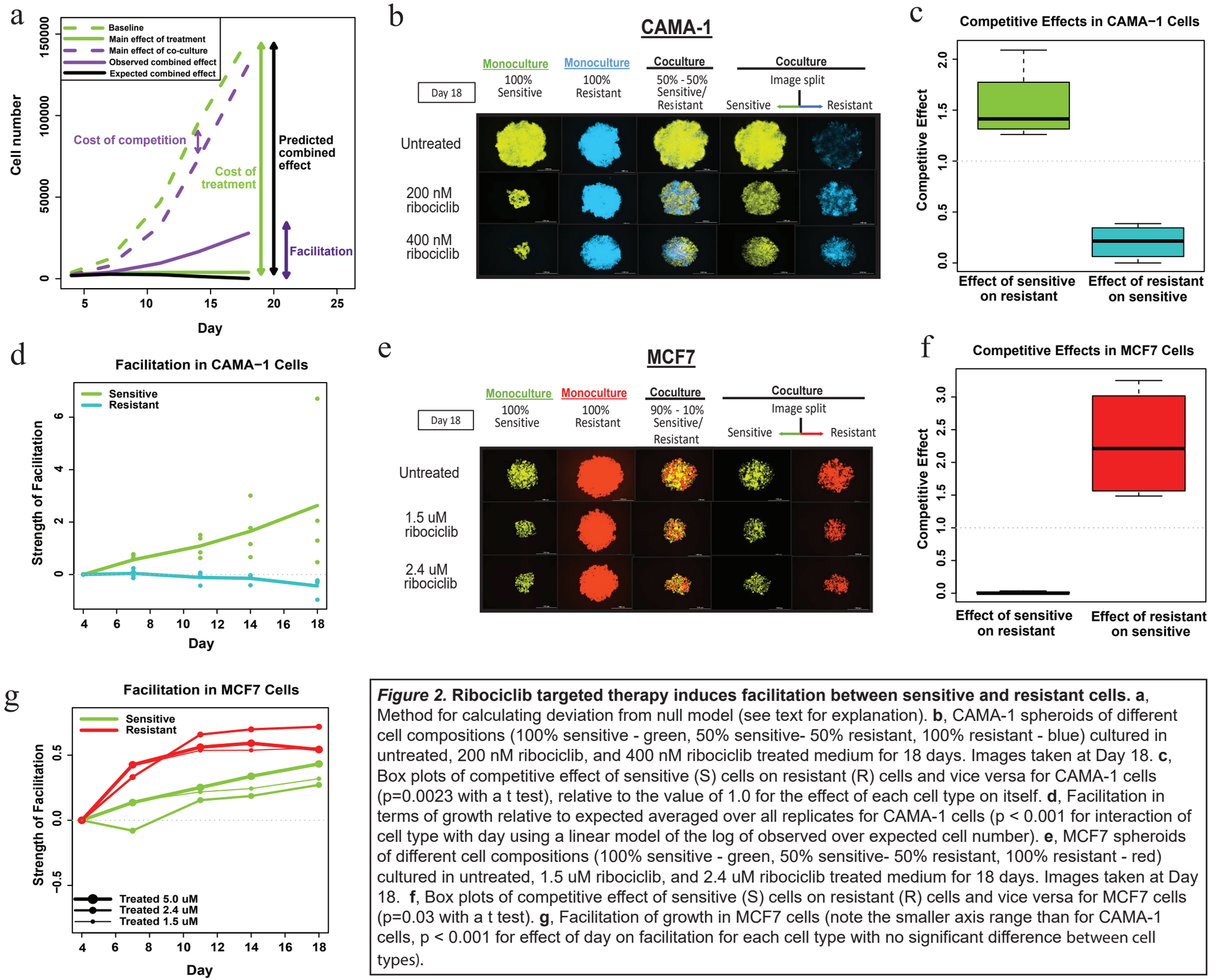


***Figure 2.*** **Ribociclib targeted therapy induces facilitation between sensitive and resistant cells. a**, Method for calculating deviation from null model (see text for explanation). **b**, CAMA-1 spheroids of different cell compositions (100% sensitive - green, 50% sensitive- 50% resistant, 100% resistant - blue) cultured in untreated, 200 nM ribociclib, and 400 nM ribociclib treated medium for 18 days. Images taken at Day 18. **c**, Box plots of competitive effect of sensitive (S) cells on resistant (R) cells and vice versa for CAMA-1 cells ($p=0.0023$ with a t test), relative to the value of 1.0 for the effect of each cell type on itself. **d**, Facilitation in terms of growth relative to expected averaged over all replicates for CAMA-1 cells ($p < 0.001$ for interaction of cell type with day using a linear model of the log of observed over expected cell number). **e**, MCF7 spheroids of different cell compositions (100% sensitive - green, 50% sensitive- 50% resistant, 100% resistant - red) cultured in untreated, 1.5 uM ribociclib, and 2.4 uM ribociclib treated medium for 18 days. Images taken at Day 18. **f**, Box plots of competitive effect of sensitive (S) cells on resistant (R) cells and vice versa for MCF7 cells ($p=0.03$ with a t test). **g**, Facilitation of growth in MCF7 cells (note the smaller axis range than for CAMA-1 cells, $p < 0.001$ for effect of day on facilitation for each cell type with no significant difference between cell types).

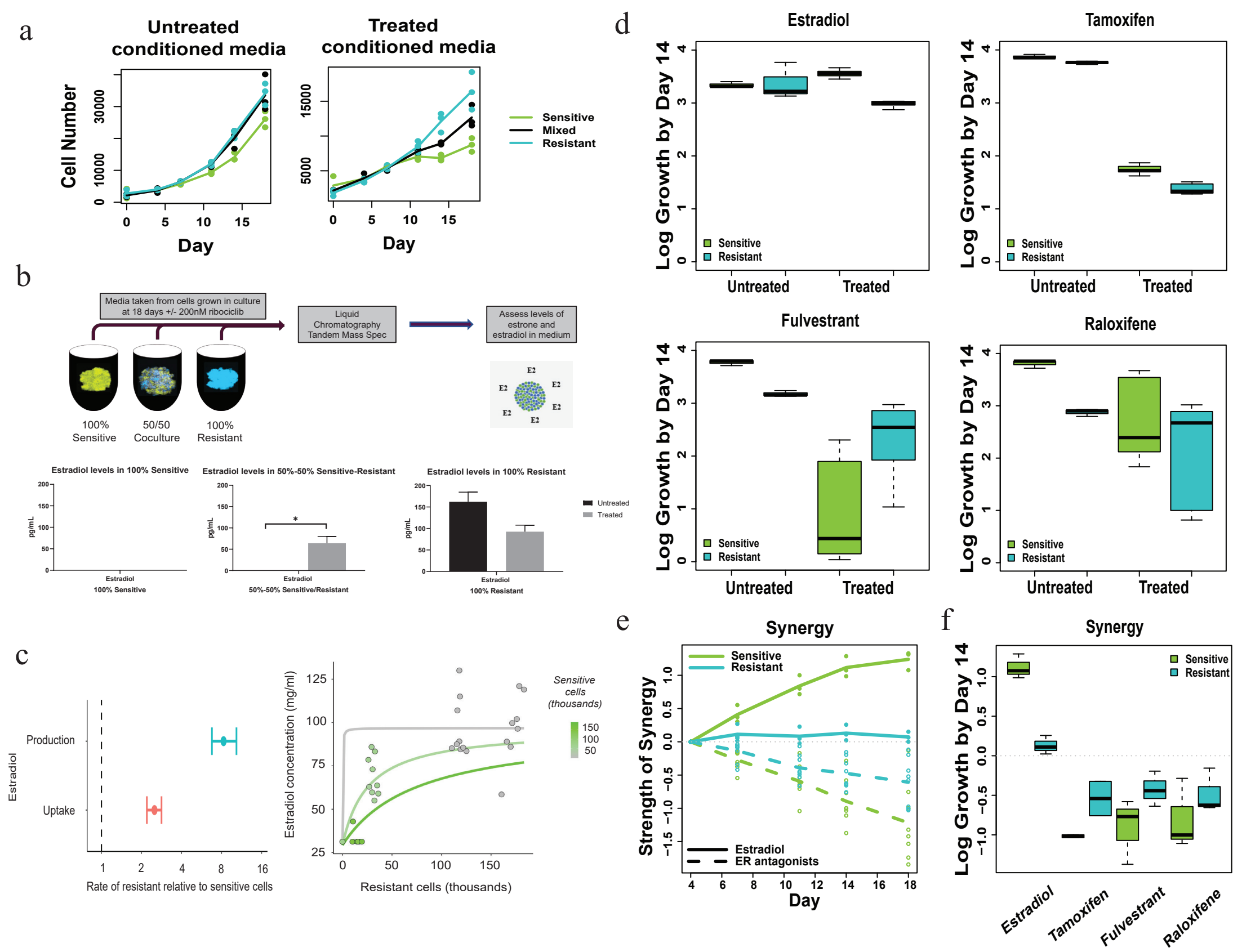


***Figure 3.*** **Underlying biological processes driving facilitation in response to ribociclib treatment. a,** Comparing growth of CAMA-1 spheroids under drug pressure with supplemented conditioned media from spheroids of different compositions. Sensitive and resistant cells were plated by the indicated composition of sensitive and resistant cells in a 3D spheroid format and underwent exposure to untreated or 400nM treated medium to produce conditioned media. 100% sensitive spheroids under drug pressure were then supplemented with different concentrations of conditioned media. Normalized cell counts of sensitive cells supplemented with untreated or treated conditioned media generated from different spheroid compositions. **b**, Liquid chromatography-tandem mass spectrometry (LC-MS/MS) assay for estradiol detection performed on CAMA-1 untreated or ribociclib 400nM treated samples of the following compositions at Day 21: 100% sensitive, 50% sensitive – 50% resistant, 100% resistant samples. **c**, Plots of estradiol production rates of CAMA-1 ribociclib sensitive and resistant cells and sensitive cell uptake of estradiol (relative to resistant cells); estradiol concentration by resistant and sensitive cell abundance **d**, CAMA-1 growth with modifier treatment in monoculture. Box plots of log of growth for sensitive and resistant cells under indicated modifier treatment (estradiol: $p < 0.0001$ for interaction between treatment and cell type indicating reduction in growth of resistant cells and increased growth by sensitive cells, tamoxifen: $p=0.006$ for interaction between treatment and cell type indicating greater reduction in growth of resistant cells, fulvestrant: $p=0.011$ for interaction between treatment and cell type indicating lower reduction in growth of resistant cells , and raloxifene: no significant interaction with growth reduced equally for the two cells types) **e**, CAMA-1 growth with combination treatment in monoculture. Comparison of observed cell growth in combination therapy with that expected under null model that assumes no interaction between the effects of the modifier treatment (estradiol, tamoxifen, fulvestrant, or raloxifene) and ribociclib ($p < 0.0001$ for sensitive cells to grow more rapidly with estradiol and $p=0.0007$ for sensitive cells to grow more slowly with ER antagonist treatment). **f**, Box plots of log of growth for sensitive and resistant cells under modifier treatment estradiol or one of three ER antagonists: tamoxifen, fulvestrant, and raloxifene) and ribociclib ($p < 0.002$ for each ER antagonist to reduce growth of sensitive cells between days 4 and 14 more than resistant cells, but no significant difference among any of the ER antagonists).

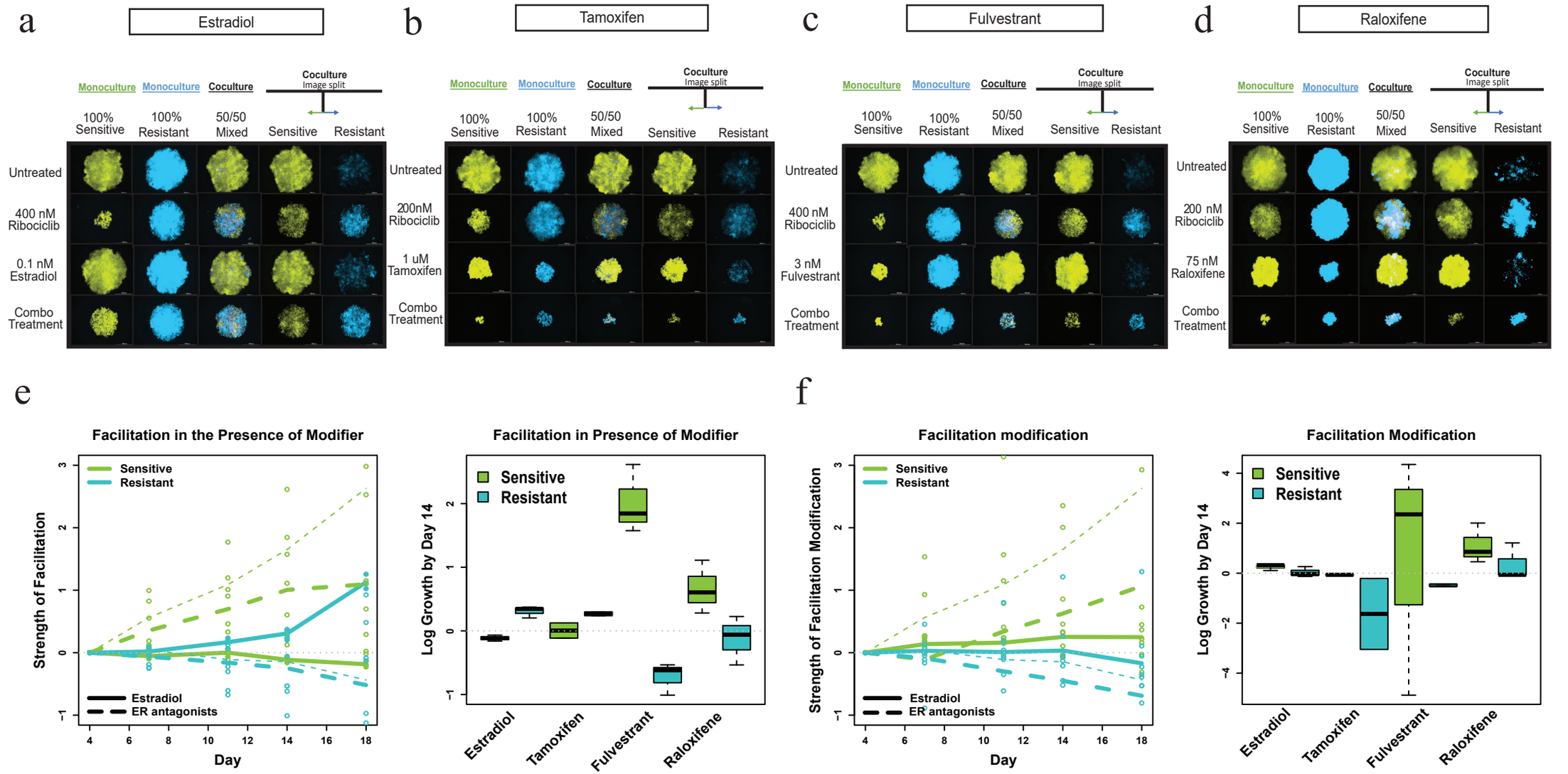


***Figure 4.*** **Modifying endocrine signaling pathways affects spheroid growth and facilitation.** CAMA-1 spheroids of different cell compositions (100% sensitive - green, 50% sensitive- 50% resistant, 100% resistant - blue) cultured in **a**, untreated, 400nM ribociclib, 0.1nM estradiol, or combination 400nM ribociclib with 0.1nM estradiol treated medium for 18 days; images taken on day 18. **b**, untreated, 200nM ribociclib, 1 uM tamoxifen, or combination 200nM ribociclib with 1 uM tamoxifen treated medium for 18 days; Images taken on day 18. **c**, untreated, 400nM ribociclib, 3nM fulvestrant, or combination 400nM ribociclib with 3nM fulvestrant treated medium for 18 days; images taken on day 18. **d**, untreated, 200nM ribociclib, 75 nM raloxifene, or combination 200nM ribociclib with 75 nM raloxifene treated medium for 18 days; images taken on day 18. **e**, Facilitation of CAMA-1 growth in coculture measured as the log of the ratio of the observed cell population to the expectation when treated with modifiers ($p < 0.0001$ for resistant cells to experience greater facilitation than sensitive cells with estradiol, and for sensitive cells to experience greater facilitation than sensitive cells when treated with ER antagonists pooled). The thin dotted lines show facilitation when treated with ribociclib for comparison; Box plots of log of growth for sensitive and resistant cells under treatment (tamoxifen effects not significantly different from estradiol, fulvestrant shows greater facilitation of sensitive cells ($p < 0.0001$) and raloxifene a smaller effect than fulvestrant ($p=0.0035$) but greater than estradiol ($p=0.0052$). **f,** Facilitation of growth in coculture measured as the log of the ratio of the observed cell population to the expectation when treated with ribociclib in the presence of a modifier ($p=0.007$ for estradiol to reduce facilitation more for resistant cells, no significant effect with the three ER antagonists pooled). The thin dotted lines show facilitation in the absence of the modifier; Box plots of log of growth for sensitive and resistant cells under combination treatments (no significant differences).

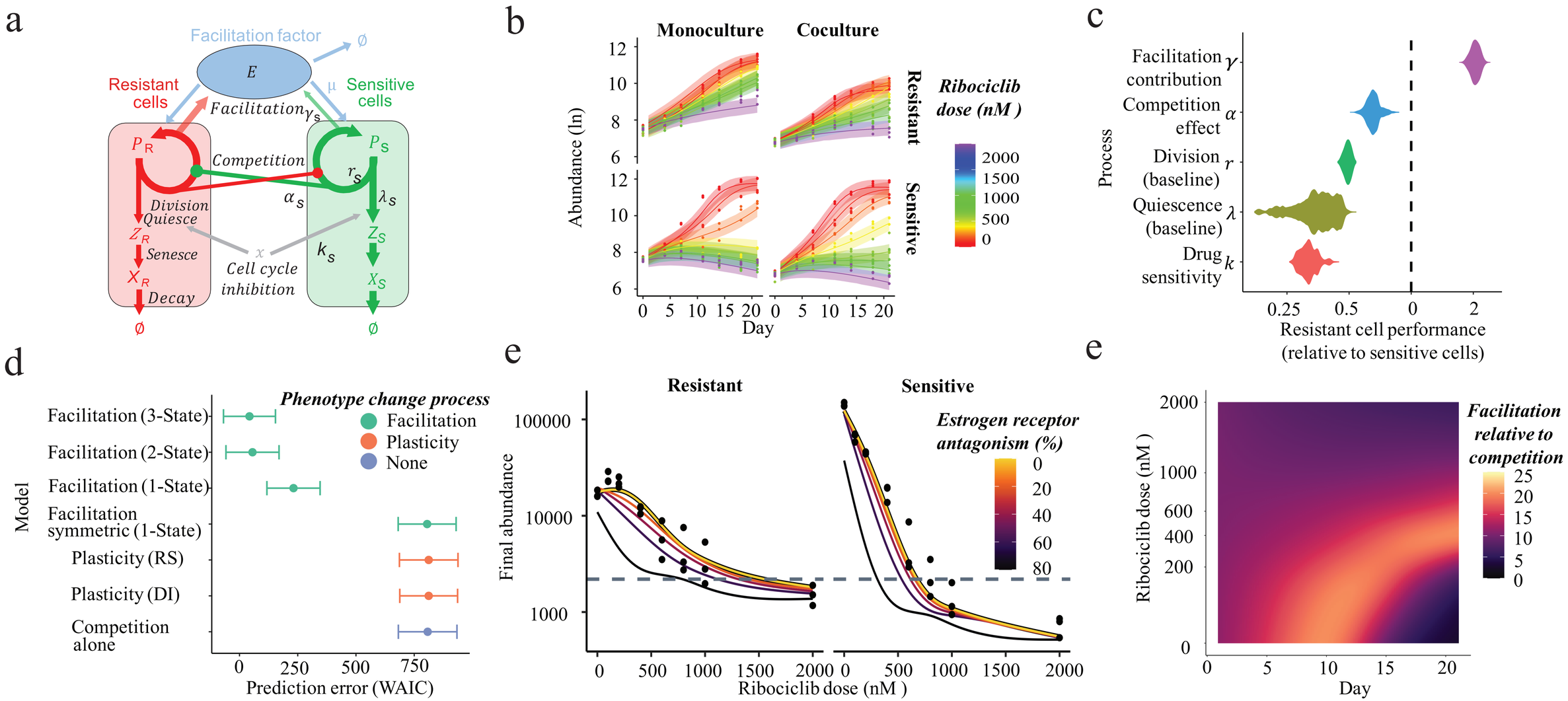


***Figure 5.*** **Measuring the strength and role of facilitation during treatment. a**, Structure of mechanistic stage –structured differential equation model of facilitation fitted to data. This describes the abundance of resistant (red) and sensitive (green) cells which compete (circle headed arrows) and also facilitate one another through the production of facilitation factor (E; estradiol; blue) used by both cell types to promote cell division. Resistant and sensitive cells transition through proliferative (P), quiescent (Z) and then senescent (X) stages. Proliferative cells enter the G1/S cell cycle checkpoint at a rate that depends on competitor abundance and facilitation factor concentration. Upon entry to the G1/S cell cycle checkpoint, cells either divide or enter the quiescent state. Cell cycle inhibitor therapy prevents accumulation of cell cycle promoting proteins, increasing the fraction of cells entering the quiescent stage, rather than dividing. **b**, Predicted spheroid growth from initial abundance for sensitive and resistant cells (rows), alone or in co-culture (columns) and across a broad range of ribociclib doses (color). Observed cell counts over time (points) are accurately predicted across all doses and cell type compositions (lines) by the facilitation model and uncertainty in model fits are captured by the 95% high credibility intervals (shaded regions). **c,** Quantification of the resistant and sensitive cells' abilities to facilitate neighboring cell growth, compete for resources, divide or quiesce in the absence of therapy and to respond to the direct impacts of treatment (drug sensitivity). Performance of resistant cells, relative to sensitive cells, is shown for each process (y axis), with the violin plots showing the range of relative performance values yielding spheroid trajectories consistent with the observed data (shaded region). Equal performance of the two cell types is signified by the vertical dashed line. **d**, Comparison of the ability of facilitation models (green) to describe the data, relative to models of phenotypic plasticity (red) or competition alone (blue). Low prediction error indicates that the model more accurately explains the spheroid growth data, whilst avoiding overfitting the data by penalizing the model likelihood based on model complexity (using WAIC: widely applicable information criterion). **e**, Prediction of impacts of blocking facilitation on sensitive and resistant cell growth in coculture, across drug dose. Data point show the observed final size of replicate spheroids across doses without facilitation blocking (100% facilitation). The thick black bordered lines show the facilitation model predictions of final size. Thinner lines show the predicted reduction in final abundance of resistant and sensitive cells achievable by reducing facilitation (brighter lines indicate greater facilitation levels (as in panel f). **f**, The role of facilitation on spheroid growth, relative to competition, across drug doses. Each point on the surface indicates a specific time and dose. The coloration shows how important facilitation is at that moment (brighter coloration indicates that facilitation is more important). The bright band shows the window of facilitation when abundance of both cell types is increasing but the carrying capacity (maximal density of the spheroid) is not reached.